**polymer**

# Solid state n.m.r. study of polymer networks based on methyl methacrylate and diethylene-glycol–bis-allyl-carbonate

## M.C.S. Perera

*School of Science, Griffith University, Nathan, Qld 4111, Australia*

## Abstract

Solid state $^{13}C$ n.m.r. measurements were carried out on polymer networks based on methyl methacrylate and diethylene-glycol–bis-allyl-carbonate. Several relaxation time parameters (rotating frame and laboratory frame proton and carbon relaxation times) were determined. Cross-polarisation times and carbon relaxation times were interpreted based on the changes in the molecular motion during the curing process. Proton relaxation times were interpreted based on the heterogeneity of the matrix. Results confirmed phase separation at complete conversion. © 1999 Elsevier Science Ltd. All rights reserved.

*Keywords:* Poly(methyl methacrylate); Poly(CR39); N.m.r.

## 1. Introduction

Copolymerisation of methyl methacrylate (MMA) and diethylene-glycol–bis-allyl-carbonate (CR39) was reported [1] to proceed in two major steps or conversion regions due to the large difference in the reactivity ratios of these two monomers. First, the predominant polymerisation of MMA with only a few CR39 units entering the molecule. Second, by the polymerisation of CR39 and cross-linking. The remaining few MMA units add to the polymer molecule during this stage. The dynamic mechanical properties [2] of the final product resulting from this copolymerisation indicate two glass transition $T_g$ regions. These two $T_g$ regions were explained by considering two phases: one with CR39-rich copolymer, which is densely cross-linked, and the second region consisting of MMA-rich copolymer which is locked in by a CR39 network.

Nuclear magnetic resonance (n.m.r.) spectroscopy is one of the few techniques available that yield motional information on the scale of molecular dimensions [3]. With the development of the high resolution techniques of cross-polarisation (CP), high power decoupling (dipolar decoupling—DD), magic angle spinning (MAS), the methods used in solution state n.m.r. have become available in the solid state. Relaxation times which can give motional frequency and amplitude information in polymer systems include $^{13}C$ spin–lattice relaxation time in the laboratory frame ($^{13}CT_1$), $^{13}C$ rotating-frame relaxation time ($^{13}CT_1\rho$), and the proton–carbon CP transfer time measured under spin lock conditions $T_{ch}$. Owing to the relatively large distances separating $^{13}C$ nuclei in natural abundance, spin diffusion does not play [4] a part in $^{13}CT_1$ and $^{13}CT_1\rho$. Further, $^{13}CT_1\rho$ has the advantage over $^{13}CT_1$, since it is sensitive to molecular motions in the 10–100 kHz frequency range. These frequencies are characteristics of the relatively long-range cooperative motions of polymer chains below $T_g$. In contrast, $^{13}CT_1$ reflects motion frequencies in the 15–75 MHz regime which deals largely with localised internal rotations. They represent motions at temperatures well above the $T_g$. At temperatures below $T_g$, the interest of $^{13}CT_1$ measurements are limited by the quasi-absence of motional modes in the higher frequency range. Thus, $^{13}CT_1\rho$ has been extensively used to study the local dynamics in bulk glassy polymers [5–7].

In solid polymers, relaxation times are not determined only by dynamic phenomena [8]. There also may exist a contribution from the static mechanism of spin diffusion. The probability for a flip flop between two opposite 1/2 spins having the same precession frequency is a decreasing function of the distance between the spins. When two proton populations have different spin temperatures at a given time, they will tend to go into a common spin temperature by spin diffusion. Spin diffusion induces a magnetisation transfer from the region where the spin temperature is initially lower to the region where the spin temperature is higher. During the measurement of $T_1$, for certain values of the

delay time $\tau$ of the $180°–\tau–90°$ sequence, there exists a situation where such magnetisation transfer could take place. Therefore, the measurement of $^1HT_1$ and $^1HT_1\rho$ is affected by the spin diffusion mechanism and spin diffusion will be efficient on length scales on the order of 100 Å and 10 Å during $^1HT_1$ and $^1HT_1\rho$ determinations respectively [9]. Thus the spin diffusion data contain information on the size of the domain in an heterogeneous system. The $^1HT_1$ and $^1HT_1\rho$ have been used to study the miscibility in polymer blends by many authors [10–12].

In the present work, solid state n.m.r. was used for investigating the reaction of MMA/CR39 and the miscibility of the components of the polymer system with different ratios of MMA/CR39. The local dynamics were investigated with measurement of carbon relaxation times and the molecular structure was studied with focus on the level of intermolecular mixing by proton relaxation times.

## 2. Experimental

### 2.1. Materials and methods

CR39, prepared at the Chiba Plant in Japan, was obtained from PPG Industries Asia Pacific Ltd. The monomer was used without any further treatment. MMA was obtained from BASF and was purified by vacuum distillation. Benzyl peroxide (BPO) was purified by twice recrystallising from methanol. Mixtures of the monomers and the initiator were prepared, as required, by weighing them accurately in a 5 ml volumetric flask. The compositions used are given in Table 1. A first set of samples was prepared by transferring about 0.3 ml of the mixture into 5 mm o.d. glass tubes. These samples were degassed just prior to the reaction, by passing nitrogen gas through for 30 min, after which they were capped to minimise the effect from oxygen. These samples were polymerised in a block heater at the required temperatures, and the cure cycles were monitored in situ using FTi.r. [1,13,14]. A second set of samples was prepared from a degassed mixture, in specially prepared kel-F inserts (to fit the n.m.r. rotors), capped and polymerised in an oven at the required temperature to the required conversion as determined from the in situ FTi.r. The set of samples in kel-F inserts were then placed in n.m.r. rotors for n.m.r. experiments.

### 2.2. N.m.r.

High-resolution solid state n.m.r. experiments were

carried out at 100 MHz for $^{13}C$ using a Varian Unity 400 spectrometer. The instrument is equipped with a high-power amplifier for proton decoupling and a Varian VT probe. Spectra were externally referenced to the aromatic peak of hexamethyl benzene (132.2 ppm). The kel-F inserts, carrying samples cured to different conversions, were placed in silicon nitride rotors with Torlon end caps. The samples were spun at speeds between 200 and 5000 Hz, depending on the extent of cure, and the sample temperature was maintained at $298 \pm 3$ K. The proton decoupling strength was approximately 60 kHz; the delay between successive pulses was 4 s and 90° pulses (5.2 $\mu$s) were performed. To enhance signal to noise $S/N$, the CP technique was applied.

Rotating- and laboratory-frame spin–lattice relaxation times for protons and rotating frame spin lattice relaxation times for carbon were obtained within the standard CP schemes. For proton relaxations a spin lock sequence with varied durations (contact times) for $T_{ch}$ and $^1HT_1\rho$ [15] and an inversion recovery sequence for $^1HT_1$ [10] were used, followed by CP and detection through carbon atoms. $^{13}CT_1\rho$ was determined using methods described in the literature using the decay of the $^{13}C$ intensities after CP contact was broken [16]. $^{13}CT_1$ data were obtained using an inversion recovery scheme without CP and a delay time of 20 s between pulses. In the $^1HT_1$ and $^{13}CT_1\rho$ measurements the contact time was generally set to 1 ms and the recycle time was set to 4 s. For each spectrum 1000–2000 scans were accumulated.

## 3. Results and discussion

### 3.1. N.m.r. chemical shift assignments

The $^{13}C$ CP/MAS n.m.r. spectrum of partially polymerised sample of the composition 2 is shown in Fig. 1a. The peaks at 19 ppm, 45 ppm, 55 ppm, 58 ppm and 180 ppm were assigned to $CH_3$, backbone quaternary carbon, $CH_3–O–$, backbone $–CH_2–$ and carbonyl carbon of PMMA respectively. The peaks at 32 ppm, 70 ppm and 156 ppm were assigned to backbone carbon atoms, $–CH_2O–$, and carbonyl carbon of poly(CR39) respectively. The peaks at 119 and 132 ppm were assigned to olefinic carbon atoms of unreacted CR39 double bonds. The peaks marked with an asterisk are spinning side bands.

The DD/MAS spectrum of the sample is shown in Fig. 1b. A comparison between peak intensities in the DD and CP spectra can be used as a qualitative measure of the local mobilities of particular structural units; higher values of DD/CP intensity ratio indicate higher mobility. The DD/CP peak intensity ratio values calculated for the carbon atoms in PMMA and poly(CR39) are given in Table 2. All spectra were normalised to the quaternary carbon at 45 ppm. All the PMMA carbon atoms have the ratio closer to unity, whereas all CR39 carbon atoms have values higher than unity. The backbone carbon of CR39 has the lowest
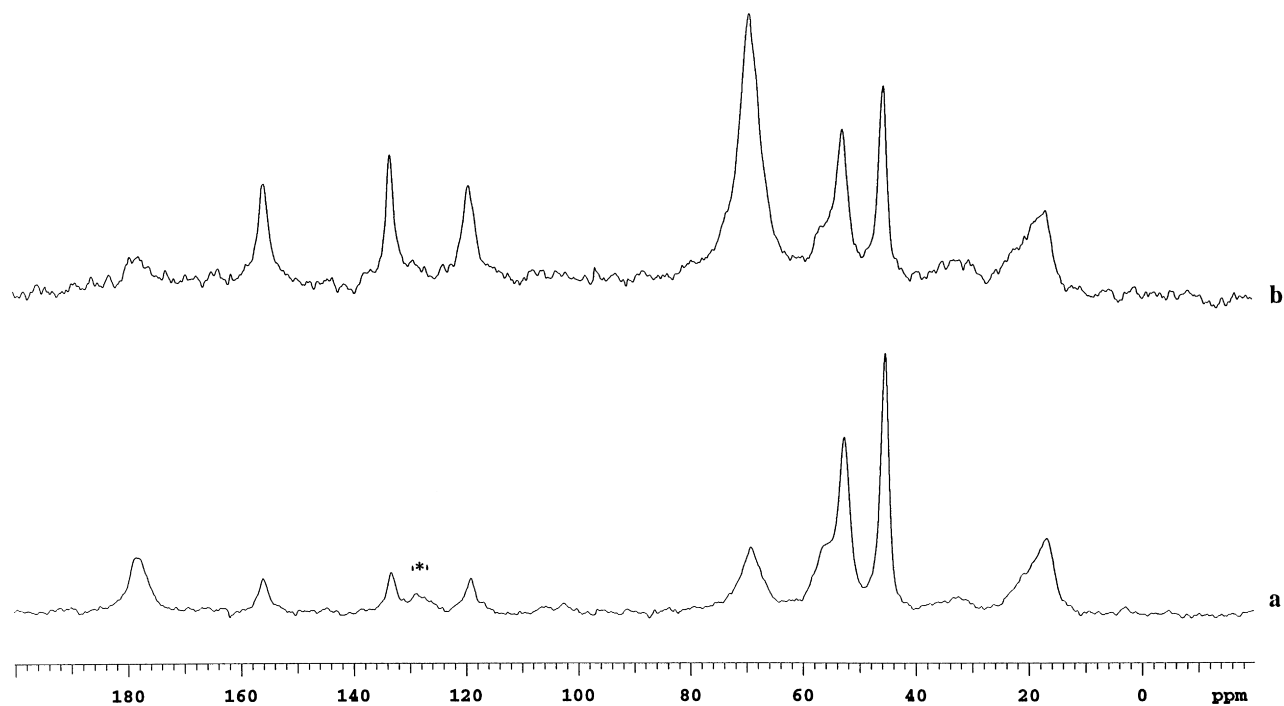
Table 1
Monomer feed compositions

| Composition name | MMA (%) | CR39 (%) |
|---|---|---|
| 1 | 75 | 25 |
| 2 | 50 | 50 |
| 3 | 25 | 75 |

Fig. 1. Solid state $^{13}C$ n.m.r. spectra of 80% total conversion sample of composition 2: (a) CP/MAS, (b) DD/MAS.

value among CR39 carbon atoms. The –CH$_2$O– and carbonyl resonances of the unreacted monomer, pendant groups of monomer linked through one double bond and cross-linked monomer of the CR39 resin could not be differentiated in the solid state $^{13}C$ n.m.r. spectrum. Therefore, the higher values of these resonances could be due to the contribution from the more mobile unreacted monomer and pendant groups. However, the peak at 30 ppm could be used to obtain some qualitative information of the mobility of the poly(CR39) molecules. The ratio values given in Table 2 indicate a lower local mobility of the PMMA molecules and higher local mobility in poly(CR39) molecules. The unreacted monomer and pendant CR39 groups are expected to plasticise both polymer molecules. A lower local mobility in PMMA molecules and higher mobility in poly(CR39) molecules indicate that there is a difference in the plasticising effect. This may arise from the difference in distribution of plasticiser in different regions of the matrix.

The DD/CP peak intensity ratio for the carbon atoms in the fully polymerised sample of composition 2 is also given in Table 2. At full conversion the local mobilities of the backbones are similar in both PMMA and poly(CR39). However, the –CH$_2$–O– still shows local flexibility compared with the other carbon atoms in the matrix.

### 3.2. CP time $T_{ch}$

The CP of $^{13}C$ nuclei by adjacent polarised protons, that is the initial build-up of the carbon magnetisation via polarisation transfer, is assumed to be controlled by a single time constant $T_{ch}$. CP occurs through a static dipolar coupling of protons and $^{13}C$ spins which are averaged out by isotropic molecular motions. Low frequency motions have the greatest effect on $T_{ch}$, where the higher the motion, the higher are the observed values. Therefore, it is believed [16] that the

Table 2
DD/CP peak ratio for carbon signals of samples of composition 2

| Carbon | Sample | |
|---|---|---|
| | 80% total conversion | fully cured |
| MMA carbonyl | 0.79 | 1.11 |
| MMA backbone –CH$_2$– | 1.35 | |
| MMA –OCH$_3$ | 1.2 | 1.1 |
| MMA backbone q-C | 1 | 1 |
| MMA methyl | 0.95 | 1.22 |
| CR39 carbonyl | 2.97 | 0.94 |
| CR39 –CH$_2$– | 5.2 | 1.6 |
| CR39 backbone carbon atoms | 2.2 | 0.94 |

$T_{ch}$ measurements provide information on near static components in the motion of a particular group.

The sharp isolated quaternary carbon resonance at 45 ppm was shown [7] to be the most consistently reliable carbon for the study of $T_{ch}$ in dimethacrylates. The value of $T_{ch}$ for this carbon with extent of cure in the comonomer system, composition 2, are plotted in Fig. 2. Total conversion is the conversion of both MMA and CR39 double bonds. It has been shown [1] that at 44% total conversion most of the MMA has reacted, whereas CR39 remains virtually unreacted, in the MMA/CR39 50/50 mixture. $T_{ch}$ values were measured above 44% conversion, as below this conversion the system is liquid and the $T_{ch}$ values are very high.

The CP mechanism available to a quaternary carbon is dependent on next-to-nearest neighbour protons and this weak interaction may, therefore, be sensitive to large amplitude motions. The constraints on group motions come about from the increasing tightness of the network, as unsaturation is consumed, and from the disappearance of free monomer, which has a plasticising effect. Vitrification is the point at which the sample $T_g$ becomes equal to the polymerisation temperature or the temperature of measurement, whichever

is lower. In this case the polymerisations were carried out using a cure cycle of 353–383 K and the n.m.r. measurements were done at 298 K. Accordingly, the $T_g$ of the mixture reaches 298 K at a total conversion of 75%. In this system, beyond 50% conversion the network begins to tighten as the CR39 commences to react. Up to 50% total conversion $T_{ch}$ was higher than that of the samples cured to higher extents. This was probably a consequence of large amplitude motions still being present at cure levels below 50% due to the plasticising effect of the CR39 molecules. As the polymerisation proceeds, the depletion of the monomer CR39, resulting in reduction in plasticisation and the formation of cross-links, will reduce motion and thus reduce $T_{ch}$. Therefore, the decline in components of the large amplitude group motions, which destroy the CP interactions, was complete well before the vitrification point.

In all the vitrified samples, $T_{ch}$ declines in the order carbonyl > quaternary C > $CH_3$ > $CH_3O$ for PMMA carbon atoms and carbonyl > backbone $C = CH_2O$ for poly(CR39) carbon atoms. The intensity of the CP interaction is short range, proportional to $r_{CH}^{-6}$. The effect is dominated by the number of nearest neighbour protons, with a diminishing effect of protons within two or three bonds
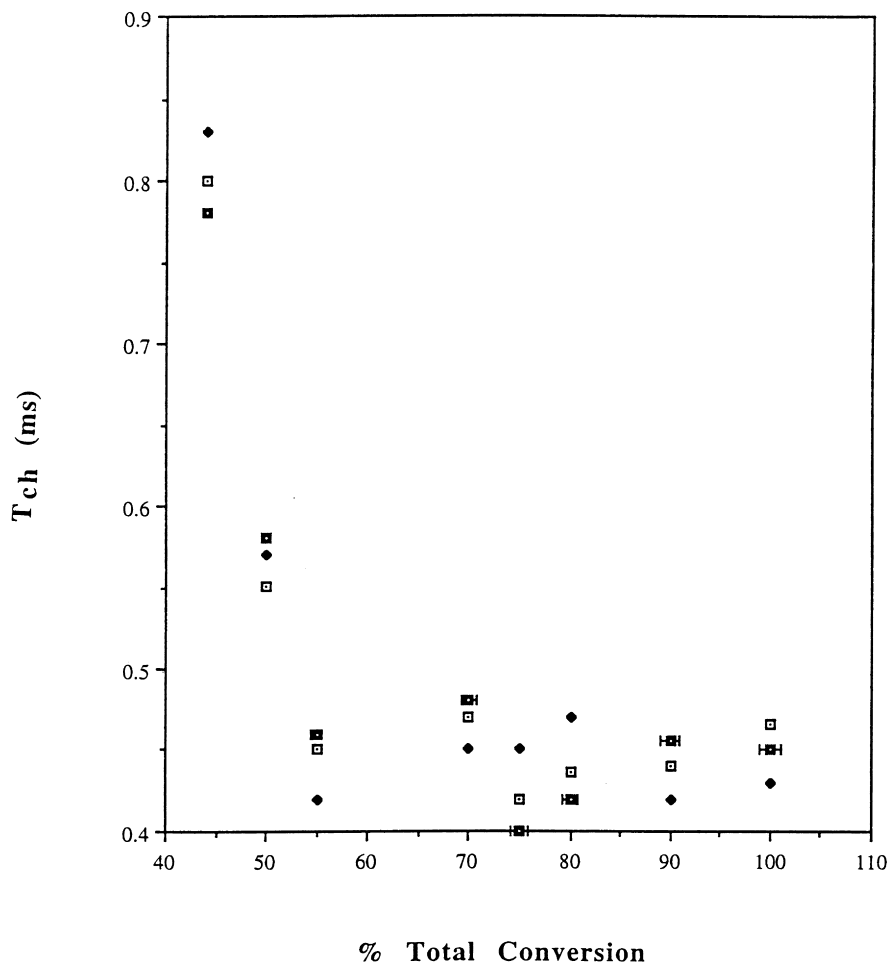


Fig. 2. CP time $T_{ch}$ versus percentage total conversion in composition 2. Different symbols indicate different polymerisation runs.

[17,18]. Rapid molecular motion attenuates the CP interactions. The above-observed order of the $T_{ch}$ values, is a result of both these effects. The $T_{ch}$ value of the carbonyl carbon of CR39 is higher than that of PMMA in the fully polymerised sample. This is due to the nearest neighbour protons for CR39 carbonyl being even further away than in PMMA carbonyl carbon. The long $T_{ch}$ for $CH_3$ in the PMMA molecule indicates inefficient CP of $^{13}CH_3$, which is consistent with its rotation. In the case of PMMA, it is well established [19] by a variety of methods that the $CH_3$ group is dynamically active at and below ambient temperatures. Scatter in the data points is too great to obtain any reasonable results to compare the $T_{ch}$ values between the different compositions.

### 3.3. $^{13}C$ spin lattice relaxation time in laboratory frame— $^{13}CT_1$

The $^{13}CT_1$ values are determined by motional components close to the Larmor frequencies, such as methyl and phenyl rotations or main chain or side chain processes of polymers at temperatures well above the glass transition temperature, i.e. in the region of few hundred megahertz. Since $^{13}CT_1$ could be determined for each carbon, it is useful in distinguishing between polymer side group dynamics and the relaxation of carbon atoms in the main chain.

Studies on vulcanisation of butyl rubber [20] and natural rubber [21,22] to cross-link levels similar to commercial vulcanisates (cross-link density up to $4.5 \times 10^{-5}$ mol g$^{-1}$) found that $^{13}CT_1$ was not sensitive to cross-link density at these low cross-link density levels. This indicates that such cross-link levels do not affect the relatively rapid segmental motions in rubbers which determine the $^{13}CT_1$ relaxation times. However, cross-link density of poly(CR39) was reported [14] to be about $3.0 \times 10^{-3}$ mol g$^{-1}$ which is about 100 times more than a commercial rubber vulcanisate.

The reaction of CR39/MMA in composition 2, beyond 44% total conversion, is mainly the reaction of CR39 double bonds. At this conversion (44%) the PMMA (lightly cross-linked) is swollen in CR39 monomer and the PMMA molecules are plasticised by the CR39 monomer molecules. Further conversion of the double bonds has two effects: introduction of more cross-links and removal of the plasticising effect of the CR39 monomer. Since $^{13}CT_1$ values are expected to be sensitive to the main chain motions, the relaxation times of the main chain quaternary carbon atom were measured in samples with different total conversions.

As the variable-temperature experiments [7,23] indicate that, for PMMA and poly-dimethacrylate, molecular motions at room temperature are in the slow motion region relative to $T_1$ minima, any increase in $^{13}CT_1$ in this system is also expected to indicate a decrease in mobility. The results indicate that $^{13}CT_1$ values are insensitive to conversion during the whole polymerisation range. At 75% total conversion, the $T_g$ of the product approaches the n.m.r. probe temperature and the $^{13}CT_1$ is expected to be insensitive beyond this point.

This insensitivity of the $^{13}CT_1$ values to conversion can be understood by considering the molecular motions that are responsible for the relaxations. In PMMA at around room temperature the methyl group reorientations are much decoupled from the extremely segmental motions below $T_g$. Hence the protons of the methyl group can move in the glassy state with part of the correlation time distribution even in the megahertz region and relax the neighbouring carbon atoms in the monomer unit despite the $r^{-6}$ proton–carbon distance dependence of relaxation rates. Owing to this methyl-dominated relaxation, there is little effect of plasticiser on the $^{13}CT_1$ values of the backbone carbon atoms. Similar findings on the plasticisation of PMMA by bisdioxane have been reported before [23].

The values of $^{13}CT_1$ for the carbon atoms in the PMMA molecule in pure PMMA and fully converted copolymer of composition 2 are given in Table 3. The $^{13}CT_1$ values for the carbon atoms in the copolymer are higher than that of pure PMMA, indicating reductions in relaxation rates which must be due to a reduction in backbone mobility. This indicates the sensitivity of the $^{13}CT_1$ values to cross-linking, which restricts molecular motion. The same scale of increase of the $^{13}CT_1$ values between the carbon atoms (doubling) suggests that this effect is due to the introduction of a restricted motion of the methyl group. However, as cross-linking is expected to reduce only the backbone mobility, the reduction in the methyl group motion should result from some other complex situation.

It has been suggested before [2] that this system ends up as a semi-interpenetrating network. The network of poly(CR39) in the interpenetrating network which traps the PMMA molecules can cause a change in the free volume and may change the methyl group motion.

Contrary to the PMMA carbon atoms, the CR39 carbon atoms show an increase in the $^{13}CT_1$ values with conversion at last stages of reaction. Restricted rotation of carbonyl

Table 3
Carbon relaxation times of PMMA carbon atoms of pure PMMA and fully cured network

| | $^{13}CT_1 \pm 20\%$ (s) | | $^{13}CT_1\rho \pm 20\%$ (ms) | | | |
|---|---|---|---|---|---|---|
| | PMMA (homo polymer) | Comp. 2 fully cured | Comp. 1 fully cured | Comp. 2 fully cured | Comp. 3 fully cured | PMMA (homo polymer) |
| $CH_3$ | 0.05 | 0.12 | 4.7 | 4.9 | 4.5 | 4.3 |
| q-C | 4.0 | 8.0 | 4.3 | 4.1 | 4.0 | 4.4 |
| $-OCH_3$ | 6.3 | 8.1 | 2.1 | 1.8 | 1.9 | 1.4 |

carbon atoms and pendant methylene carbon is observed as these units take part in cross-linking. This indicates a phase separation where some of the CR39 molecules exist without the interference of the methyl rotation of the PMMA molecules.

### 3.4. $^{13}C$ spin lattice relaxation time in the rotating frame—$^{13}CT_1\rho$

The measurement of $^{13}CT_1\rho$ was performed by an experiment where the spin lock contact was established and then terminated followed by allowing the $^{13}C$ polarisation to decay in its own rotating field for a determined interval. This was terminated by switching off the carbon field, restoring the proton field and acquiring the data. The decay in the $^{13}C$ magnetisation in its rotating field was assumed to be controlled by a single relaxation time, $^{13}CT_1\rho$. The $^{13}CT_1\rho$ is sensitive to molecular motions in the 10–100 kHz frequency range, characteristic for relatively long-range cooperative motions of a polymer chain below the $T_g$.

The change in the $^{13}CT_1\rho$ of the quaternary carbon with total conversion is given in Fig. 3. The most striking feature is the restriction of the relaxation mechanism after vitrification: beyond 80% total conversion the tightening of the network commences. This is the conversion where about 60% of CR39 is polymerised. A homo polymerisation study [14] of CR39 showed that the conversion at which the network tightening commenced was about 60%. Prior to 80% total conversion, although polymerisation and cross-linking of CR39 occurs, the flexible nature of the ethylene glycol units in the pendant groups plasticises the PMMA molecules. Therefore, even though a network is formed during this conversion range, the network is flexible enough to keep the $^{13}CT_1\rho$ values low. $^{13}CT_1\rho$ and its frequency domain are particularly sensitive to plasticisation [24].

The $^{13}CT_1\rho$ values for the fully polymerised CR39/MMA mixtures of different compositions are given in Table 3. The
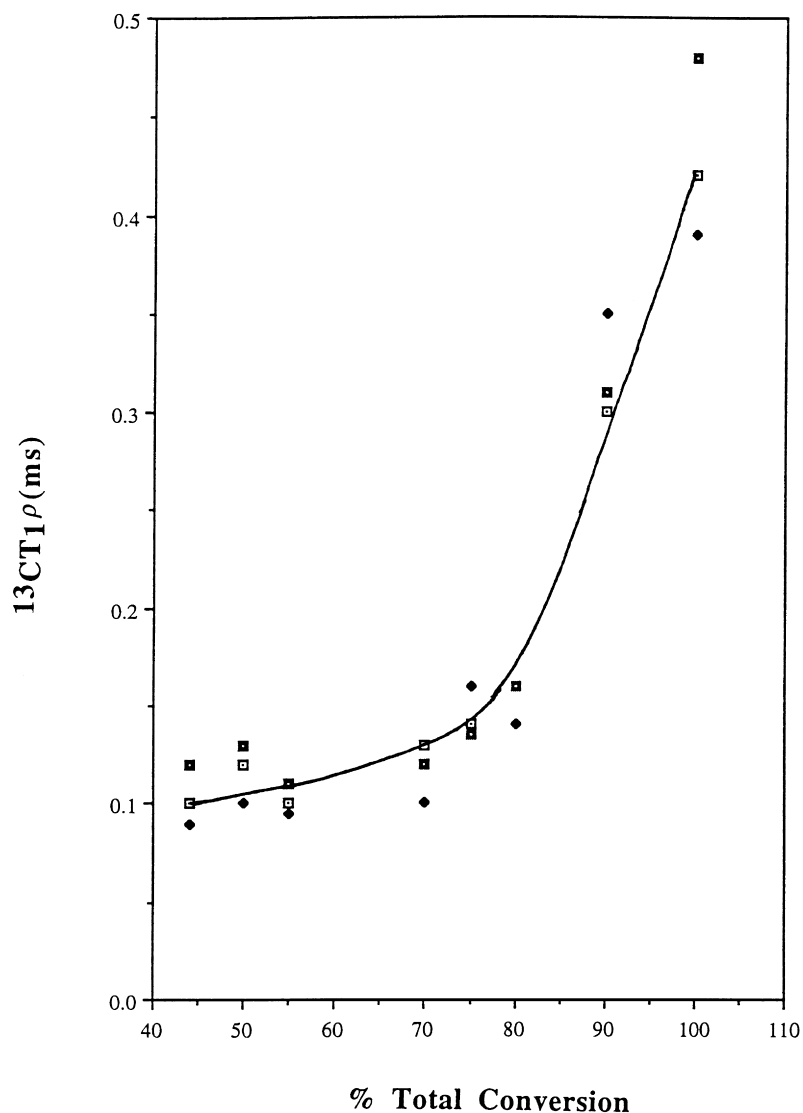


Fig. 3. $^{13}C$ spin lattice relaxation time, $^{13}CT_1\rho$ versus percentage total conversion in composition 2. Different symbols indicate different polymerisation runs.

PMMA carbon relaxations are found to be similar for all compositions. The formation of two phases was considered [2] to explain the dynamic mechanical analysis data of these systems (Fig. 4). As the polymerisation proceeds, initially the MMA undergoes polymerisation to form PMMA with few CR39 molecules in the structure. These CR39 molecules contribute to a lightly cross-linked network; this stage will be referred to as the intermediate polymerisation stage. At this stage this network is swollen in the free CR39. The mobility of PMMA will depend on the cross-linking network caused by poly(CR39) in that phase. The amount of CR39 in the PMMA-rich phase during further polymerisation depends on two factors: the degree of cross-linking and the amount of free CR39 in the system at the intermediate stage. These factors have two opposing effects. When there is more CR39 in the feed composition, more CR39

molecules enter into the polymer at the intermediate stage. The higher the CR39 in the PMMA molecules, the higher is the cross-link density and lower is the volume swollen. In contrast, the higher the amount of free monomer at the intermediate stage, the higher is the amount swollen at the equilibrium level of swelling. For example, it is possible that composition 1 will not reach equilibrium. However, as the polymerisation proceeds, the cross-link density in the PMMA-rich phase will increase and this will cause an amount of free CR39 to be rejected from the swollen network. At a certain cross-link density (different conversions in different compositions) the amount of free monomer in the swollen network is similar in the three compositions. Therefore, at the final conversion, we could expect the PMMA-rich phase to have the same cross-link density in all three compositions and thus similar $^{13}CT_{1}\rho$ values.
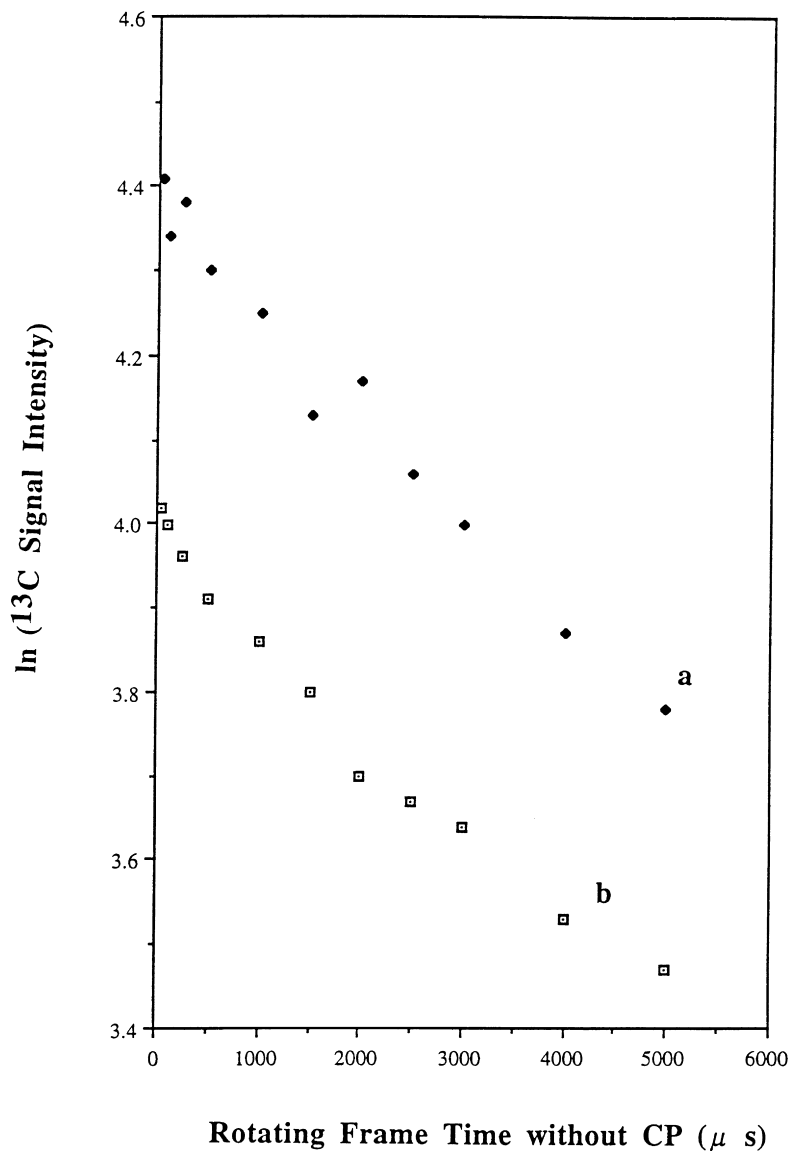


Fig. 4. ln($^{13}$C signal intensity of PMMA q-carbon) versus rotating frame time without CP contact ($\mu$s): (a) homo polymer PMMA; (b) fully converted composition 2.

On the other hand, it is possible that non-motional spin processes may contribute [25], which would decrease the sensitivity of $^{13}CT_{1\rho}$ to change in molecular motions. In some PMMA blends, the lack of sensitivity in $^{13}CT_{1\rho}$ to detect the molecular motions has been explained [12] by considering the possible mobility of the $CH_3$ group below $T_g$. This mobility can relax the neighbouring carbon atoms causing the relaxation time measurements to be insensitive. However, the observation of the change in $^{13}CT_{1\rho}$ of other carbon atoms with conversion indicates that these molecular motions do not originate from the methyl group motions. Similar effects have been reported [7] in polymerisation of dimethacrylates.

### 3.5. Proton spin lattice relaxation times $^1HT_{1\rho}$ (rotating frame) and $^1HT_1$ (laboratory frame)

More detailed information about the miscibility of two polymer components could be obtained from proton relaxation behaviour. The $^1HT_{1\rho}$ values were measured by analysing the decay of the carbon magnetisation for long contact times in a CP experiment. The measurement through the carbon spins has the advantage that the $T_{1\rho}$ values for protons near carbon atoms with different chemical shifts can be determined separately. By this method it is possible to determine the $^1HT_{1\rho}$ for both components of the matrix. The protons of the two components of the compatible blend have the same $^1HT_{1\rho}$ if the molecules are in contact on an intimate molecular distance $L$ over which proton can effectively diffuse in a given time $t$ related by [25].

$\langle L^2 \rangle \sim (t/T^2) l_0^2$ where $l_0$ is the distance between protons and $T_2$ is the proton spin–spin relaxation or hopping rate. The available time for spin diffusion $t$ is equal to the spin–lattice relaxation time $^1HT_1$ or $^1HT_{1\rho}$. If the chains are intimately and homogeneously mixed, spin diffusion occurs quickly among the chemically different constituents, and a single value of $^1HT_{1\rho}$ is determined through analysis of the decay rates for all carbon atoms. If the chains do not interact on the molecular level, different proton $T_{1\rho}$ values are observed for the carbon atoms corresponding to the different polymers.

The results of the determination of $^1HT_{1\rho}$ values for the carbon atoms in the samples of composition 2 cured to differing extents and fully polymerised PMMA and partially

and fully polymerised CR39 are given in Table 4. The $^1HT_{1\rho}$ values for 80% and fully polymerised CR39 are similar within experimental error. At this conversion most of the CR39 molecules have entered the polymer and the unreacted double bonds are mainly pendant groups. Plasticisation by these pendant groups does not affect the $^1HT_{1\rho}$ values. The $^1HT_{1\rho}$ decay of the nuclei of homo polymers is shown in Fig. 5. The nuclei from both polymers could be characterised by a single $^1HT_{1\rho}$ at room temperature, within experimental error. These results are consistent with data usually observed on amorphous glassy polymers. They are characterised by values of 13 ms and 4 ms for PMMA and poly(CR39) respectively. Even though there is evidence for local heterogeneities in poly(CR39) from kinetic analysis, the $^1HT_{1\rho}$ is not sensitive enough to observe that heterogeneity.

The $^1HT_{1\rho}$ relaxation behaviour for PMMA carbon atoms and poly(CR39) carbon atoms in the 80% total conversion sample of composition 2 is similar. This is also shown in Fig. 5 as a single graph. The intensity dependence of carbon atoms in both PMMA and poly(CR39) is an exponential function of the delay time in the contact time, CP pulse sequence. It is characterised by a $5 \pm 1$ ms $^1HT_{1\rho}$. This value of $^1HT_{1\rho}$ obtained for both PMMA and poly(CR39) carbon atoms at 80% total conversion is between the values of the homo polymers. This indicates molecular-level mixing between PMMA and poly(CR39) at this polymerisation conversion.

The $^1HT_{1\rho}$ relaxation behaviour for PMMA carbon atoms and poly(CR39) carbon atoms in the fully converted sample of composition 2 is shown in Fig. 6. At complete conversion two different values of $^1HT_{1\rho}$ were obtained: $13 \pm 1$ ms and $3.5 \pm 1$ ms for PMMA carbon atoms and poly(CR39) carbon atoms respectively. This indicates a phase separation on a domain size scale of 20–30 Å. All samples show single-exponential decay with contact time in the experiment. This indicates that even if there is a phase separation, as discussed in the previous work [2], only after the networks are locked in, the spin diffusion mechanism provides evidence of this phase separation phenomena. At 44% total conversion, part of the unreacted CR39 molecules and pendant CR39 groups are distributed homogeneously in the PMMA network. As discussed above, when these remaining

Table 4
$^1HT_{1\rho}$ (ms) values ($\pm$ 20%) for carbon atoms in partially and fully cured CR39, copolymer composition 2 and PMMA

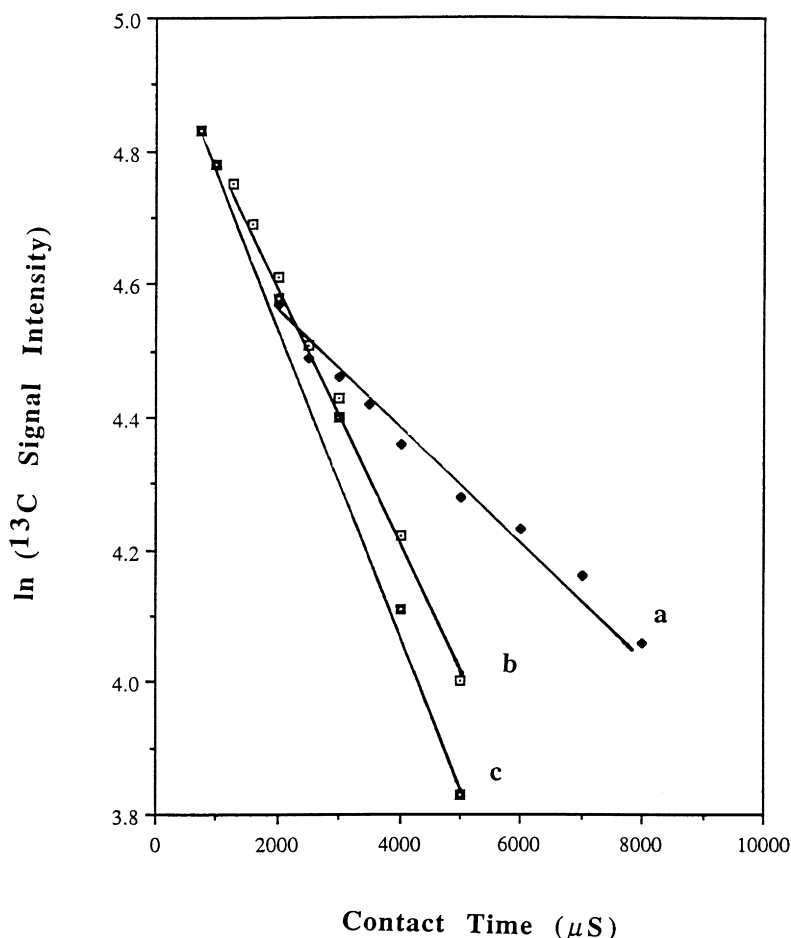| | PMMA carbon atoms | | | | Poly(CR39) carbon atoms | | | |
|---|---|---|---|---|---|---|---|---|
| | $CH_3$ | q-C | $CH_3$–O– | carbonyl | backbone C | $-CH_2$–O– | carbonyl | double bond C |
| Comp. 2 80% cured | 4.6 | 4.2 | 5.0 | 5.1 | 4.9 | 4.8 | 6.2 | 5.3 |
| Comp. 2 fully cured | 11.7 | 10.6 | 11.4 | 14.7 | 3.0 | 3.1 | 3.3 | |
| PMMA | 14.3 | 11.9 | 12.8 | 13.3 | | | | |
| CR39 80% cured | | | | | 2.1 | 2.2 | 3.3 | 3.3 |
| CR39 fully cured | | | | | 3.6 | 3.5 | 3.3 | |

Fig. 5. ln($^{13}$C signal intensity) versus contact time ($\mu$s) of: (a) backbone CH$_2$ of PMMA molecules in homo polymer PMMA; (b) backbone CH$_2$ of PMMA molecules in 80% converted composition 2; (c) backbone carbon of fully converted CR39.

double bonds react, at one critical stage, the free CR39 molecules are rejected from PMMA-rich phase. This results in a phase separation. The values of $^1HT_{1\rho}$ of PMMA measured in the fully cured sample are only slightly less than the value of the pure PMMA (13 ms) and are similar in all three compositions. As the $^1HT_{1\rho}$ values of a miscible blend depend [26] on the volume fractions of the components, this indicates that the PMMA-rich component has a very small amount of CR39 and is similar in all three compositions. If the linear model is used, the mole fraction of PMMA in the PMMA-rich component is calculated to be 0.98. This confirms the phase separation of the PMMA-rich component in the fully cured network.

The laboratory frame proton relaxation $^1HT_1$ may be used to indicate miscibility on a larger scale (200–300 Å) and that the domain sizes are smaller than 200 Å. But in this system these results cannot be used as there is no difference between the $^1HT_1$ values of the two homo polymers.

## 4. Conclusions

The partially polymerised sample of MMA/CR39 mixture was found to be inhomogeneous with respect to the distribution of the monomer CR39. This is indicated by the difference in local mobilities of backbone carbon atoms in the two polymers as shown in the peak ratio of the DD/CP spectra.

The long amplitude motions of the PMMA molecule were found to diminish long before the vitrification set in.

The $^{13}CT_1$ values of the carbon atoms of PMMA were not found to be sensitive to detect changes in molecular motions due to the motion of the methyl group. However, at very high conversion, the poly(CR39) carbon atoms show an increase indicating that they are not influenced by the PMMA methyl group motions. This is interpreted as being due to phase separation.

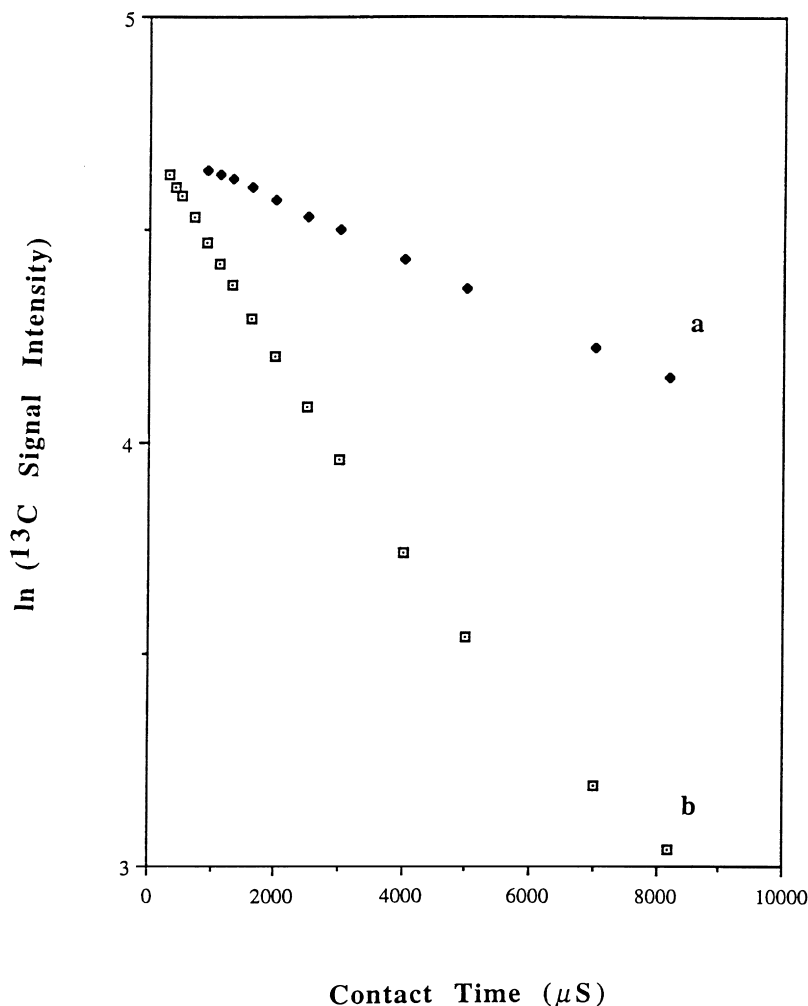$^{13}CT_{1\rho}$ values of both polymer components were sensitive to motions after the vitrification.

Fig. 6. ln($^{13}$C signal intensity) versus contact time ($\mu$s) of fully converted composition 2: (a) backbone CH$_2$ of PMMA; (b) backbone carbon of poly(CR39).

Proton relaxation time measurements indicate good mixing of the two polymers up to about 80% total conversion and phase separation at full conversion.

## References

[1] Hill DJT, Perera MCS, Pomery PJ, Joseph E. Polymer 1997;38:695.
[2] Hill DJT, Perera MCS, Pomery PJ. Polymer (in press).
[3] Havens JR, Koenig JL. Appl Spectrosc 1983;37:226.
[4] Vanderttart DL, Garroway AN. J Chem Phys 1979;71:2773.
[5] Garbow JR, Schefar J. Macromolecules 1987;20:819.
[6] Dickinson LC, Morjanelli P, Chu CW, Petrovic Z, Macknight WJ, Chien JCW. Macromolecules 1988;21:338.
[7] Allen PEM, Simson GP, Williams DRG, Williams EH. Eur Polym J 1986;22:549.
[8] Laupretre F. Prog Polym Sci 1990;15:425.
[9] Abraham A. The principles of nuclear magnetism. New York: Oxford University Press, 1961.
[10] Stejskal EO, Schaefer J, Sefcik MD, Mckay RA. Macromolecules 1981;14:275.
[11] Parmer JF, Dickinson LC, Cheers JCW, Porter RS. Macromolecules 1989;22:1078.
[12] Schantz S. Macromolecules 1997;30:1419.
[13] Hill DTT, O'Donnell JH, Perera MCS, Pomery PJ. Eur Polym J 1997;33:1353.
[14] Hill DJT, O'Donnell JH, Perera MCS, Pomery PJ. Eur Polym J 1997;33:649.
[15] Sullivan MJ, Maciel GE. Anal Chem 1982;54:1615.
[16] Schaefer J, Stejskal EO, Buchdahl R. Macromolecules 1977;10:384.
[17] Alemany LB, Grant DM, Pugmire RJ, Alger TD, Zilm KW. J Am Chem Soc 1983;105:2133.
[18] Alemany LB, Grant DM, Pugmire RJ, Alger TD, Zilm KW. J Am Chem Soc 1983;105:2147.
[19] McCrum NG, Read BE, Williams G. Anelastic and dielectric effects in polymer solids. New York: Wiley, 1967.
[20] Komoroski RA, Mandelkern L. J Polym Sci Polym Lett Ed 1976;14:253.
[21] Zaper AM, Koenig JL. Rubb Chem Technol 1987;60:252.
[22] Zaper AM, Koenig JL. Rubb Chem Technol 1987;60:278.
[23] Edzes HT, Veeman WS. Polym Bull 1981;5:255.
[24] Bellfiore LA, Henricks PM, Massa DJ, Zumbulyadis N, Rothwell WP, Cooper SL. Macromolecules 1983;16:1744.
[25] Fleming WW, Lyerla JR, Yannoni CS. In: Randal JC, editor. NMR and macromolecules, ACS Symposium Series, vol. 247. Washington, DC: ACS, 1984:83.
[26] McBrierty VJ, Douglass DC, Kwei TK. Macromolecules 1978;11:1265.